



**HAL**  
open science

# Dual frequency laser with two continuously and widely tunable frequencies for optical referencing of GHz to THz beatnotes

Gwennaël Danion, Cyril Hamel, Ludovic Frein, François Bondu, Goulc'Hen Loas, Mehdi Alouini

► **To cite this version:**

Gwennaël Danion, Cyril Hamel, Ludovic Frein, François Bondu, Goulc'Hen Loas, et al.. Dual frequency laser with two continuously and widely tunable frequencies for optical referencing of GHz to THz beatnotes. *Optics Express*, 2014, 22 (15), pp.17673. 10.1364/OE.22.017673 . hal-01081126

**HAL Id: hal-01081126**

**<https://hal.science/hal-01081126>**

Submitted on 7 Nov 2014

**HAL** is a multi-disciplinary open access archive for the deposit and dissemination of scientific research documents, whether they are published or not. The documents may come from teaching and research institutions in France or abroad, or from public or private research centers.

L'archive ouverte pluridisciplinaire **HAL**, est destinée au dépôt et à la diffusion de documents scientifiques de niveau recherche, publiés ou non, émanant des établissements d'enseignement et de recherche français ou étrangers, des laboratoires publics ou privés.

# Dual frequency laser with two continuously and widely tunable frequencies for optical referencing of GHz to THz beatnotes

Gwennaél Danion,\* Cyril Hamel, Ludovic Frein, François Bondu, Goulchen Loas and Mehdi Alouini

Institut de Physique de Rennes, UMR 6251, CNRS, Université de Rennes1 Campus de Beaulieu, 35042 Rennes Cedex, France.

\*gwennael.danion@univ-rennes1.fr

**Abstract:** A dual-frequency 1.55  $\mu\text{m}$  laser for CW low noise microwave, millimeter and submillimeter wave synthesis is demonstrated, where frequency stabilization is possible on each wavelength independently. The solid state Er:Yb laser output power is 7 mW. The amplitude noise is  $-150$  dBc/Hz at 1 MHz offset frequency. In free running regime, the frequency noise is  $3.10^5/f$  Hz/sqrt(Hz) (800 Hz on a  $1\mu\text{s}$  timescale), better than commercial fibered or semi-conductor sources at this wavelength.

©2014 Optical Society of America

**OCIS codes:** (140.3580) Lasers, solid-state; (060.5625) Radio frequency photonics; (040.2235) Far infrared or terahertz.

---

## References and links

1. S. Tonda-Goldstein, D. Dolfi, A. Monsterleet, S. Formont, J. Chazelas, and J. P. Huignard, "Optical signal processing in radar systems," *IEEE Trans. Microw. Theory Tech.* **54**(2), 847–853 (2006).
2. I. Mukhopadhyay, "Tunable THz sources and their applications," *Int. J. Infrared Millim. Waves* **24**(7), 1063–1080 (2003).
3. T. Hidaka, S. Matsuura, M. Tani, and K. Sakai, "CW terahertz wave generation by photomixing using a two-longitudinal-mode laser diode," *Electron. Lett.* **33**(24), 2039–2040 (1997).
4. G. Ducournau, P. Szriftgiser, T. Akalin, A. Beck, D. Bacquet, E. Peytavit, and J. F. Lampin, "Highly coherent terahertz wave generation with a dual-frequency Brillouin fiber laser and a 1.55  $\mu\text{m}$  photomixer," *Opt. Lett.* **36**(11), 2044–2046 (2011).
5. A. Rolland, G. Loas, M. Brunel, L. Frein, M. Vallet, and M. Alouini, "Non-linear optoelectronic phase-locked loop for stabilization of opto-millimeter waves: towards a narrow linewidth tunable THz source," *Opt. Express* **19**(19), 17944–17950 (2011).
6. G. Danion, G. Loas, L. Frein, C. Hamel, A. Carre, S. Bouhler, M. Vallet, M. Brunel, A. Rolland, M. Alouini, F. Bondu, F. Cleva, J. P. Coulon, M. Merzougui, A. Brillat, A. Beck, G. Ducournau, M. Zaknoute, C. Coiron, X. Wallart, E. Peytavit, T. Akalin, J. F. Lampin, G. Pillet, L. Morvan, G. Baili, and J. Bourderionnet, "High spectral purity microwave and terahertz oscillator," *IEEE/IFC Symposium* 40–42 (2013).
7. F. Bondu, M. Brunel, M. Vallet, G. Loas, M. Romanelli, and M. Alouini, "Device for producing high frequencies by means of light frequency beating," US patent 20130100973A1 (2013).
8. M. Notcutt, L. S. Ma, J. Ye, and J. L. Hall, "Simple and compact 1-Hz laser system via an improved mounting configuration of a reference cavity," *Opt. Lett.* **30**(14), 1815–1817 (2005).
9. G. Karlsson, N. Myrén, W. Margulis, S. Taccheo, and F. Laurell, "Widely tunable fiber-coupled single-frequency Er-Yb:glass laser," *Appl. Opt.* **42**(21), 4327–4330 (2003).
10. B. Jacobsson, V. Pasiskevicius, and F. Laurell, "Tunable single-longitudinal-mode ErYb:glass laser locked by a bulk glass Bragg grating," *Opt. Lett.* **31**(11), 1663–1665 (2006).
11. S. Taccheo, G. Sorbello, G. Della Valle, P. Laporta, G. Karlsson, F. Laurell, W. Margulis, and S. Cattaneo, "Generation of micro- and THz-waves at 1.5  $\mu\text{m}$  by dual-frequency Er: Yb laser," *Electron. Lett.* **37**(24), 1463–1464 (2001).
12. M. Alouini, M. Brunel, F. Bretenaker, M. Vallet, and A. Le Floch, "Dual tunable wavelength Er,Yb:glass laser for terahertz beat frequency generation," *IEEE Photon. Technol. Lett.* **10**(11), 1554–1556 (1998).
13. S. Taccheo, P. Laporta, S. Longhi, O. Svelto, and C. Svelto, "Diode-pumped bulk erbium-ytterbium lasers," *Appl. Phys. B* **63**(5), 425–436 (1996).
14. P. Laporta, S. Taccheo, S. Longhi, O. Svelto, and C. Svelto, "Erbium-ytterbium microlasers: optical properties and lasing characteristics," *Opt. Mater.* **11**(2-3), 269–288 (1999).
15. L. Richter, H. Andelberg, M. Kruger, and P. McGrath, "Linewidth determination from self-heterodyne measurements with subcoherence delay times," *IEEE J. Quantum Electron.* **22**(11), 2070–2074 (1986).

16. A. Rolland, G. Ducournau, G. Danion, G. Loas, M. Brunel, A. Beck, F. Pavanello, E. Peytavit, T. Akalin, M. Zaknounge, J. F. Lampin, F. Bondu, M. Vallet, P. Szriftgiser, D. Bacquet, and M. Alouini, "Narrow linewidth tunable terahertz radiation by photomixing without servo-locking," *IEEE Trans. Terahertz Sci. Technol.* **4**(2), 260–266 (2014).
17. G. Pillet, L. Morvan, D. Dolfi, J. Schiellein, and T. Merlet, "Stabilization of new generation solid-state dual-frequency laser at 1.5  $\mu\text{m}$  for optical distribution of high purity microwave signals," *IEEE Microwave Photonics* 163–166 (2010).
18. F. Hartmann and F. Stoeckel, "Stabilité de fréquence et pureté spectrales des lasers," *J. Phys. Colloq.* **39**(C1), 31–36 (1978).
19. M. Alouini, M. Vallet, M. Brunel, F. Bretenaker, and A. Le Floch, "Tunable absolute-frequency laser at 1.5  $\mu\text{m}$ ," *Electron. Lett.* **36**(21), 1780–1782 (2000).
20. R. W. P. Drever, J. L. Hall, F. V. Kowalski, J. Hough, G. M. Ford, A. J. Munley, and H. Ward, "Laser phase and frequency stabilization using an optical resonator," *Appl. Phys. B* **31**(2), 97–105 (1983).

## 1. Introduction

Generation of microwave to sub millimeter monochromatic CW radiation with large and continuous frequency tuning offers many applications in spectroscopy, telecommunication, radar systems, time-frequency metrology or millimeter radio astronomy [1–3]. Photomixing two optical frequencies at 1.55  $\mu\text{m}$  on a InGaAs-InP unitravelling carrier photodiode (UTC-PD) [4] allows a frequency tuning on a terahertz bandwidth, which is a major advantage to fully electrical techniques. Currently, the state of the art technique for achieving THz high spectral purities through photomixing is the opto-electronic phase locked loops (OEPLL) [5]. In this case, the frequency difference of two laser lines is optically down converted to an intermediate frequency locked to an electrical reference. The frequency noise of the electrical oscillator is then up-scaled with the ratio of the beatnote frequency to the RF reference frequency. To overcome this drawback, we have proposed few years ago a technique where both laser lines are simultaneously referenced to two different resonances of a single Ultra Low Expansion (ULE) Fabry-Perot cavity [6,7]. This approach should improve the phase noise of the beat note as compared to that of the up-scaled electrical references. Nevertheless, it requires laser sources whose linewidth on a 1  $\mu\text{s}$  time scale is narrower than the reference cavity line which is of the order of 10 kHz [8]. In addition, the two wavelengths must be independently tunable with a coarse tuning, in order to adjust the THz beatnote frequency, and a fine voltage-controlled tuning in order to servo-lock each wavelength on one longitudinal mode of the ULE cavity. These requirements are well addressed by single-mode solid state lasers [9,10]. Nevertheless, the use of two independent lasers leads to a large drift of the free running beatnote. A dual frequency laser offers a much lower drift due to common environment variations for the two optical lines [11]. Moreover, a two-polarization architecture [12] provides perfectly orthogonal modes, making it easy to separate and recombine them at will. In this paper, we detail the design of a dual frequency laser sustaining the oscillation of two frequencies that are widely, continuously and independently tunable. In addition, we show that the noise characteristics of this dual frequency laser are compatible with the requirements for optical referencing each wavelength onto a ULE cavity [6].

## 2. Laser design

The dual-frequency laser architecture is shown on Fig. 1. It consists in a 7 cm long plano/concave cavity. The active medium is a 1.5-mm-long phosphate glass co-doped with a 1.65% weight fraction of  $\text{Er}_2\text{O}_3$  and a 22% of  $\text{YbO}_3$ . The input coupler M1, directly coated on the external side of the active medium has a transmission of 95% at 980 nm and 0.1% around 1550 nm, i.e., at the oscillating wavelengths. The resonator is closed by the output coupler M2 with a maximum reflectivity of 99.5% at 1550 nm. The 4 cm radius curvature is chosen as short as possible according to mechanical constraints in order to facilitate a single longitudinal mode operation. A birefringent  $\text{YVO}_4$  crystal (5x5x20mm, AR at 1550 nm), cut at 45°, inside the laser cavity yields a beam separation of 2 mm for the ordinary and extraordinary lasing modes (labeled *o* and *e* in Fig. 1): the two modes share the same optical path between the output curved mirror and the downstream part of the cavity, whereas they are separated between the rest of the cavity and the flat input coupler. The input 980 nm pump

is also split into two separated pump beams with a second YVO<sub>4</sub> crystal (5x5x19.76mm, AR at 980 nm). The pump consists of a single mode 980 nm fiber Bragg grating stabilized diode providing 800 mW. This guarantees a low laser threshold and avoids partition noise encountered with multimode pump. Although it has been shown that a 40  $\mu\text{m}$  pump beam radius offers the maximum slope efficiency [13], we found that the best compromise in order to ensure simultaneous oscillation on both modes is 50  $\mu\text{m}$ .

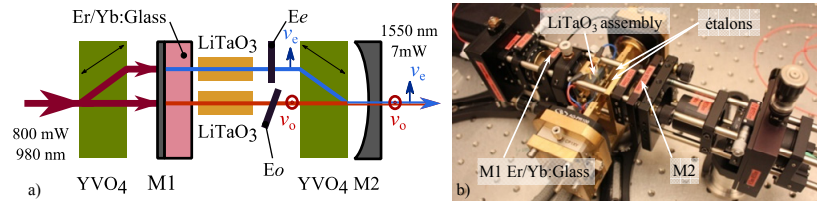


Fig. 1. (a) Schematic section diagram of the two-tunable frequencies laser. M1: input coupler, M2: 99.5% output coupler, o: ordinary axis, e: extraordinary axis. LiTaO<sub>3</sub>: electro-optic crystals of lithium tantalate, E (e-o): etalon, YVO<sub>4</sub>: birefringent crystal. (b) Photograph of the dual frequency laser with two independently tunable frequencies.

The single longitudinal mode operation is obtained on each axis by 40- $\mu\text{m}$  thick etalons (*E<sub>o</sub>* and *E<sub>e</sub>*) coated on both sides to reflect 30% of the intensity at 1550 nm. The coarse tunability of each wavelength is realized independently by tilting the etalons. High precision piezo rotations (5  $\mu\text{rad}$  adjustment resolution) enable frequency tuning by steps of the 1.7 GHz corresponding to the free spectral range (FSR) of the laser cavity. The laser emission is thus tunable between 1541 nm and 1548 nm (see Fig. 2), leading to a beat note tunable from DC to 900 GHz. Let us mention that the tuning range is limited, in our case, by the moderate thickness of the active medium unlike in [12], which enables higher pumping rate and consequently better intensity and phase noise performances.

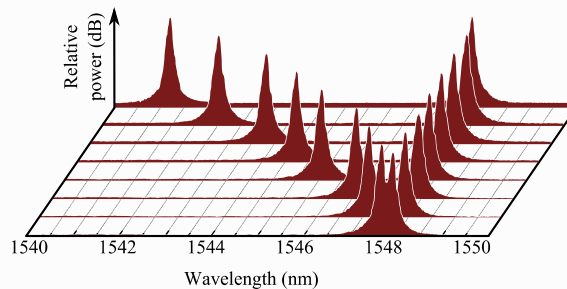


Fig. 2. Optical spectrum for different tilt of the etalon on the ordinary axis. The wavelength difference between the two axes can be adjusted over 7 nm span. The optical spectrum analyzer resolution is 0.07 nm.

For fine tuning and frequency servo-locking purpose, we need a voltage control of both frequencies. We thus inserted into the cavity two identical electro-optical crystals, one per polarization axis. These crystals are 8 mm long lithium tantalate (LiTaO<sub>3</sub>, x<sub>1</sub> cut, labeled LTO) whose both sides are antireflection coated at 1550 nm. Chrome-gold electrodes are deposited on the two opposite sides along the crystal parallel to the optical axis. These electrodes are separated by 2 mm corresponding to the crystal thickness. In order to maximize the electro-optic efficiency for both axes and because the polarizations of the two axes are crossed, these two crystals have to be oriented at 90° with respect to each other.

At  $\lambda = 1550$  nm, it leads to an electro-optic gain of 1.1 MHz/V. Since the laser cavity FSR is 1.7 GHz, more than 1000 volts would be required to obtain a continuous sweep of each frequency. A solution to circumvent this drawback is to take advantage of the thermo-optic effect expected to be 600 MHz/°C. Indeed, we can notice that only 3° are necessary to sweep

the 1.7 GHz FSR of the laser. The combination of both effects permits to tune continuously each frequency with a precision of about 1 MHz, limited by the temperature regulation precision. It is worthwhile to mention that, this laser being designed for dual optical referencing, the thermo-optic gain, which has a sub-Hz time constant, is intended to compensate for the residual drift of each laser frequency, whereas the electro-optic gain, whose time constant is below 1  $\mu$ s, will be used for compensating the fluctuations of each laser frequency.

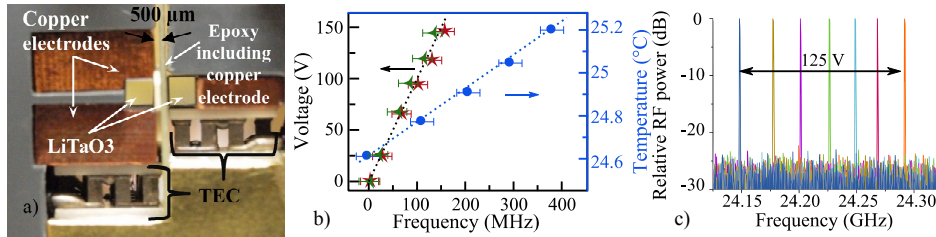


Fig. 3. (a). Macro photograph of the electro-optic mechanical assembly, TEC: Peltier effect cooler. In this view, the two optical axes of the laser (o and e) are centered on the two LiTaO<sub>3</sub> crystals and oriented along the normal of the view. (b). Optical frequency tuning. The red and green plots represent the electrooptic gain for the extraordinary and ordinary laser axis respectively. The blue plot represents the thermo optic gain reported here for the extraordinary axis only. (c) Illustration of electrooptic beat note tuning at low frequency.

Figure 3(a) is a picture of the transverse implementation of the two electro optics. The main constraints are the small spacing of the two electrodes, as well as the electrical and thermal insulations between the 2 crystals to reduce cross talks to negligible levels. In order to minimize optical diffraction losses of each mode, we estimated that the maximum thickness of insulation between the two crystals should be thinner than 1 mm. Consequently, we used a 400  $\mu$ m thick plate of epoxy for both thermal and electrical insulations. A copper track is etched on one of its sides enabling electrical contact with the inner vertical electrode of the electro-optic (see Fig. 3(a)). To further decrease thermal crosstalk, a 100  $\mu$ m thick insulation dielectric material of 0.05 W/(m.K) is inserted vertically between the two electro-optic crystals opposite to the etched side of the epoxy plate. We verified experimentally that the electro-optic and thermo-optic gains. The measurement has been performed on a beat note tuned at 6 GHz (Fig. 3(b)). A linear behavior is measured for both voltage or temperature variations, and excellent concordances are observed with the expected values, for both laser axes. Moreover, we have measured that the voltage cutoff frequency of the LTO input is higher than 10 MHz. Each LTO is controlled in temperature by a Peltier element. The blue line in Fig. 3(b) shows the frequency change when the temperature set to only one Peltier element is modified. We also verified that there is negligible crosstalk between each crystal. Consequently, for each laser axis, we benefit from both high bandwidth electro optic effect and high gain but low bandwidth thermo-optic effect. Finally, by adjusting the orientations of the etalons and the temperature and voltage applied to the LTO crystals, any optical frequency difference can be attained for both polarizations over a range of 900 GHz.

The entire laser is displayed on Fig. 1(b). Its total output power is around 7 mW, slightly dependent of the etalons tilt. According to the numerous elements inside the cavity and the low gain of the active medium (around 10%), a lot of care is taken in minimizing intracavity losses. Moreover, the choice of the transmission of the output coupler is determinant to ensure at the same time high output power and high pumping rate. Indeed, the laser must operate far enough from threshold for reducing its relative intensity noise [14]. This tradeoff is found for an output coupler transmission of 0.5%, leading to a pumping rate of 4.

In order to fully analyze the noise characteristics of our laser, its beam is coupled to a polarization maintaining fiber and a 26 GHz bandwidth InGaAs photodiode connected to a spectrum analyzer. We first measure the linewidth of the beat-note signal after a polarizer oriented at 45°. A typical result is illustrated in Fig. 4 for a beat note of 12.5 GHz. A beat-

note linewidth of 30 kHz is measured (Fig. 4(a)) with a resolution bandwidth (RBW) of 30 kHz and a sweep time measurement of 0.05 s. This result proves that the intrinsic free running beatnote remains narrow despite the insertion of additional optical elements in the cavity as compared to [12] or [13]. We also observed a beat note drift as low as 5 MHz per minute (see Fig. 4(b)).

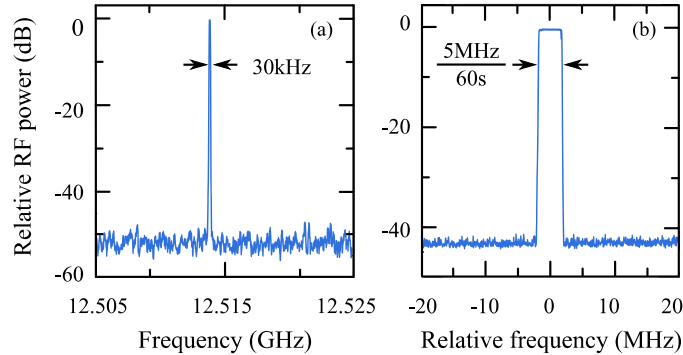


Fig. 4. (a) Electrical spectrum of a beat note at 12.5 GHz (RBW 30 kHz, sweep time 0.05 s). (b) Max hold measurement of the drift of that beat-note on 1 minute (RBW 100 kHz).

We finally characterized the relative intensity noise (RIN) as well as the phase noise of this laser in the free running regime. In solid state lasers, the RIN being shot noise limited above 10 MHz we use a 100 MHz bandwidth InGaAs photodiode followed by a homemade low noise transimpedance amplifier. The experimental RIN spectrum obtained when the two orthogonal laser modes are projected at  $45^\circ$  is reported in Fig. 5(a). It shows an excess noise at the two relaxation oscillation (RO) frequencies around 100 kHz. The optical power of the two modes being identical at the laser output, the small shift between the two RO peaks evidences the slight difference of intracavity losses and pumping rate between the two oscillating modes. As expected, above 1 MHz, the RIN drops down rapidly to reach the shot noise level (here related here to the 0.3 mW optical power on the photodiode).

Figure 5(b) represents the frequency noise of the beat note ( $\Delta\nu = \nu_e - \nu_o$ ) and of one of the optical carriers ( $\nu_e$  here, the frequency noise of  $\nu_o$  being the same). On the one hand,  $\Delta\nu$  is demodulated after the 26 GHz high speed photodiode both in phase and in quadrature (I and Q) using an electrical spectrum analyzer (Rohde and Schwarz FSV 3.6). The phase noise is then reconstructed numerically. On the other hand, the phase noise of one optical carrier is analyzed using a self-heterodyne method [15], where one arm of the Mach-Zehnder interferometer contains an acousto-optic modulator at 80 MHz, whereas the second arm includes a fiber delay of 700 m. At the output, the beat signal at 80 MHz is detected by the 26 GHz photodiode, and then demodulated into I and Q quadratures. Finally, the 80 MHz phase noise is translated into laser frequency noise. In Fig. 5(b), the red line represents the phase noise when the laser beat note  $\Delta\nu$  is adjusted to 1.5 GHz. The green line represents the phase noise of the optical carrier. We can note that the phase noises (beatnote and carrier) of our laser prototype are almost identical. We have also plotted in this figure the phase noise of the optical carrier when the pumping beam is transverse-multimode, showing significant noise degradation induced by transverse-mode partition noise [16,17]. This justifies the fact that we implemented to our final prototype a transverse-monomode pumping scheme, which leads to phase noises much better than that of commercial semiconductor lasers or fibered lasers. The laser linewidth depends on the measurement time,  $\tau$ , and is related to the phase noise. The Allan standard deviation [18] in our case is found to be  $800 \sqrt{(\tau/1\mu\text{s})}$  Hz, well within our 10 kHz target. The Allan standard deviation corresponds to 5 kHz on a  $\sim 1/(30 \text{ kHz})$  time scale, in agreement with the electrical spectrum analyzer rough estimate. The overall performances obtained here in terms of noise and frequency agility makes this dual frequency laser well

suites to servo lock each of its wavelengths to a single ULE cavity with a linewidth as low as 1 kHz and a feedback loop of a 1 MHz bandwidth.

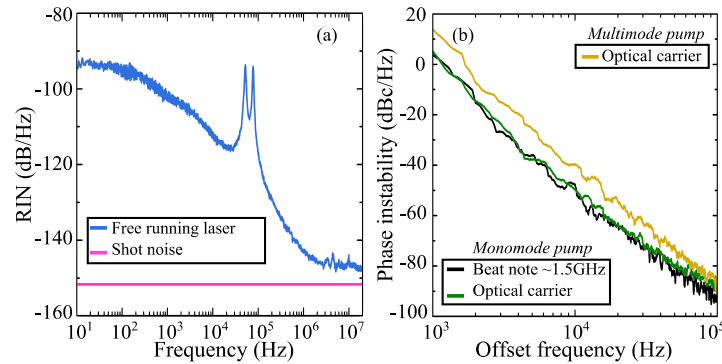


Fig. 5. (a) Relative intensity noise in free running regime (blue line). Shot noise level calculated with 0.3 mW of optical power (pink line). (b) Yellow line: phase noise of one optical carrier among two when the pumping beam is transverse-multimode. Green line: phase noise of one optical carrier when the pumping beam is transverse-monomode. Black line: Phase noise of the beatnote between the two optical carriers.

### 3. Conclusion

In this paper we describe how we have developed a compact two continuously and widely tunable frequency laser at 1.5  $\mu\text{m}$  that is devoted for optical referencing of GHz to THz beatnotes. Each optical frequency is continuously tunable over 7 nm around 1545 nm. The continuous tuning of each frequency is obtained by combining three independent effects (i) a coarse tuning by steps of 1.7 GHz by tilting an intracavity etalon, (ii) an intermediate but continuous tuning within each FSR of the laser cavity through thermo-optic effect (600 MHz/C), and (iii) a fine and high cutoff frequency tuning through electro-optic effect (1.1 MHz/V). The beat note frequency is thus continuously tunable from DC to 900 GHz. The performances of such a laser in terms of noise and frequency control are shown to be perfectly adapted to stabilize independently each frequency to different resonances of a single ULE cavity or even to acetylene ro-vibrational resonances [19]. This laser is indeed designed to be implemented in a larger experiment for THz metrology [6]. Furthermore, the proposed architecture is well suited for direct Pound-Drever-Hall stabilization [20] without external phase modulation due to the intracavity LTO crystals whose modulation bandwidth is designed to be 10 MHz. Further characterization of the optical lines in terms of drift and jitter, when considered independently, will be conducted. Finally, the mean wavelength at 1.5  $\mu\text{m}$  of this laser is compatible with photomixing technology using InGaAs-InP unitravelling carrier photodiodes (UTC-PD) [3] that will enable us to radiate the low phase noise THz radiations.

### Acknowledgments

This work is supported by Agence Nationale de la Recherche (OSMOTUS ANR-2011 - BS0301001). We thank our colleagues, Loïc Morvan and Daniel Dolfi, from THALES Research and Technology for providing the active gain medium and Grégoire Pillet, Antoine Rolland, Steve Bouhier and Anthony Carré for fruitful discussion.